UC Berkeley
UC Berkeley Previously Published Works

Title
Direct Transformation of SiH4 to a Molecular L(H)2Co ▫ Si ▫ Co(H)2L Silicide Complex

Permalink
https://escholarship.org/uc/item/4pc173nw

Journal
Journal of the American Chemical Society, 145(5)

ISSN
0002-7863

Authors
Handford, Rex C
Nguyen, Trisha T
Teat, Simon J
et al.

Publication Date
2023-02-08

DOI
10.1021/jacs.2c11569

Copyright Information
This work is made available under the terms of a Creative Commons Attribution License, available at https://creativecommons.org/licenses/by/4.0/

Peer reviewed

eScholarship.org Powered by the California Digital Library
University of California

Direct Transformation of SiH_4 to a Molecular $L(H)_2Co{=}Si{=}Co(H)_2L$ Silicide Complex

Rex C. Handford,[†] Trisha Nguyen,[≡] Simon J. Teat,[‡] R. David Britt,[≡] T. Don Tilley[†,*]

[†]Department of Chemistry, University of California, Berkeley, Berkeley, California 94720, United States
[≡]Department of Chemistry, University of California, Davis, Davis, California 95616, United States
[‡]Advanced Light Source, Lawrence Berkeley National Laboratory, Berkeley, California, 94720, United States

ABSTRACT: Despite the critical importance of silicide phases (M_xSi_y) in industry and academia, investigations of molecular analogues remain constrained by a lack of accessible, rational routes to well-defined examples of these species. In this work, the synthesis of bimetallic molecular silicide complexes was undertaken, based on use of multiple Si-H activations in SiH_4 at the metal centers of 14-electron {L}Co^I fragments (L = Tp", *tris*-3,5-(diisopropylpyrazolyl)borate; [$BP_2{}^{tBu}Pz$], $PhB(CH_2P'Bu_2)_2(Pz)$). Upon exposure of $(Tp"Co)_2(\mu\text{-}N_2)$ (**1**) to SiH_4, a mixture of $(Tp"Co)_2(\mu\text{-}H)$ (**2**) and $(Tp"Co)_2(\mu\text{-}H)_2$ (**3**) was formed and no evidence for Si—H oxidative addition products was observed. In contrast, [$BP_2{}^{tBu}Pz$]-supported Co complexes led to Si—H oxidative additions with generation of silylene and silicide complexes as products. The base-stabilized silylene [$BP_2{}^{tBu}Pz$]$(H)_2$CoSiHPh(DMAP) (**7**; DMAP = 4-dimethylaminopyridine) was obtained by treatment of [$BP_2{}^{tBu}Pz$]Co(DMAP) (**6**) with $PhSiH_3$. The reaction of ([$BP_2{}^{tBu}Pz$]$Co)_2(\mu\text{-}N_2)$ (**5**) with SiH_4 gave the dicobalt silicide complex [$BP_2{}^{tBu}Pz$]$(H)_2Co{=}Si{=}Co(H)_2$[$BP_2{}^{tBu}Pz$] (**8**) in high yield, representing the first direct route to a symmetrical bimetallic silicide. The effect of the [$BP_2{}^{tBu}Pz$] ligand on Co—Si bonding in **7** and **8** was explored by analysis of solid-state molecular structures and density functional theory (DFT) investigations. Upon exposure to CO or DMAP, **8** converted to the corresponding [$BP_2{}^{tBu}Pz$]$Co(L)_x$ adducts (L = CO, x = 2; L = DMAP, x = 1) with concomitant loss of SiH_4, despite the lack of significant Si—H interactions in the starting complex. With heating to 60 °C, **8** reacted with MeCl to produce small quantities of Me_xSiH_{4-x} (x = 1–3), demonstrating functionalization of the μ-silicon atom in a molecular silicide to form organosilanes.

INTRODUCTION

Binary transition-metal silicide phases (M_xSi_y) are critical solid-state materials used in microelectronic technologies,[1–3] and as catalysts that enable important industrial and technological transformations of silicon-containing materials.[4–6] Most significantly, the Direct Process is practiced on an enormous, worldwide industrial scale to convert elemental silicon and MeCl to Me_2SiCl_2.[7] This process involves Si–Cl and Si–C bond formations on the surface of a copper silicide and enables the silicones industry.[7–10] Interestingly, various transition-metal silicide nanoparticles are used to grow silicon nanowires, created *via* decomposition of molecular silane species at the silicide surface.[6,11,12] Thus, metal silicide catalysts exhibit surface chemistry that promotes useful bond-forming and bond-breaking reactions of silane derivatives.

Metal silicides may be more generally useful in silicon technology; however, the search for new chemical transformations is hindered by a lack of information relating to the reaction mechanisms that occur on a silicide surface, and the specific surface structures involved in this chemistry. In this regard, well-defined molecular models for metal silicide reactive sites should reveal atomic-level insights into the reactivity associated with strong metal-silicon bonding interactions.

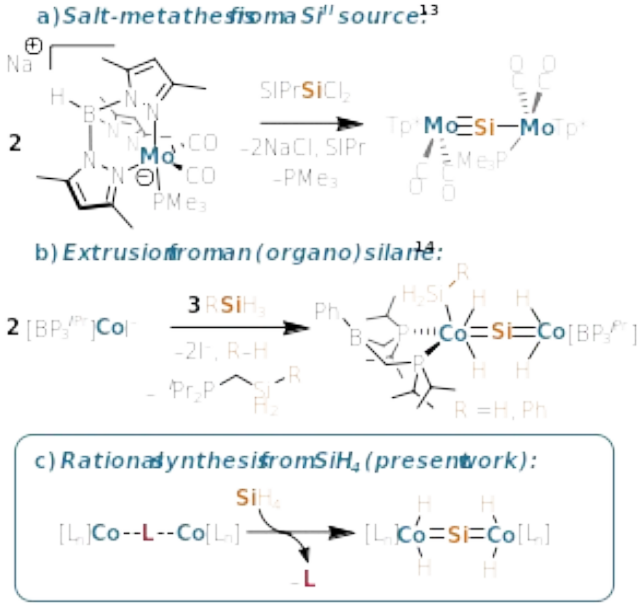

Figure 1. Methods to access bimetallic silicide complexes. a) Synthesis of an unsymmetrical silicide by salt-metathesis of a low-valent silicon source. b) Synthesis of unsymmetrical silicides by μ-silicon atom extrusion from (organo)silanes. c) Rational synthesis of a silicide by activation of SiH_4.

Until very recently,[13,14] molecular metal silicides were represented by a small range of metal-silicon carbonyl clusters generated in complex product mixtures by reaction of a metal carbonyl with organosilanes or SiH_4. For example, MacKay and Nicholson reported the *spiro*-silicon cluster $[(OC)_8Fe_2]_2(\mu_4\text{-}Si)$ from reaction of SiH_4 with $Fe_2(CO)_9$,[15] whereas Si_2H_6 and $Co_2(CO)_8$ generate complex mixtures that include $[(OC)_7Co_2]_2(\mu_4\text{-}Si)$, $[(OC)_4Co](\mu_4\text{-}Si)[Co_3(CO)_9]$, and

$[(OC)_4Co]_2(\mu_5\text{-}Si)_2[Co_4(CO)_{11}]$.[16] In 2018, Filippou *et al.* described a specialized route to a bimetallic silicide, by reaction of (SIPr)$SiBr_2$ (SIPr = 1,3-*bis*-(2,6-diisopropylphenyl)-4,5-dihydroimidazol-2-ylidene) with two equivs of $[Tp^*Mo(CO)_2(PMe_3)]^-$ (Tp* = *tris*-(3,5-dimethylpyrazolyl)borate) to produce $Tp^*(OC)_2Mo{\equiv}Si{-}Mo(CO)_2(PMe_3)Tp^*$ (Figure 1a). This complex, referred to by the authors as a metallasilylidyne, was reduced to a dianionic $\{Mo{=}Si{=}Mo\}^{2-}$ analogue.[17] Despite these interesting examples, there remains a need for rational synthetic routes to well-defined molecular silicides, and reactivity studies that characterize the chemical properties for isolated M_xSi_y units.

Our research group recently reported a route to bimetallic silicides involving cleavage of all bonds to silicon in the simple silanes SiH_4 and $PhSiH_3$.[14] Specifically, a precursor to the 14-electron fragment $[BP_3^{iPr}]Co^I$ ($[BP_3^{iPr}]$ = $[PhB(CH_2P^iPr_2)_3]^-$) was observed to react with SiH_4 or $PhSiH_3$ to give unsymmetrical silicides $[BP_2^{iPr}](RSiH_2)(H)_2Co{=}Si{=}Co(H)_2[BP_3^{iPr}]$ ($[BP_2^{iPr}]$ = $PhB(CH_2P^iPr_2)_2$; R = H, Ph), where the μ-silicon atom is derived from the parent silane (Figure 1b). These reactions represent the first examples of well-defined silicide "extrusion" from simple silanes. However, this synthetic route appeared to involve a complex process relying on fragmentation of the $[BP_3^{iPr}]$ ligand with concomitant formation of a cobalt-bound silyl ligand.

Until now, there has been no general synthetic route to bimetallic molecular silicides *via* the direct conversion of a silane. However, known silane activations that involve "double Si–H" bond cleavage[18–21] suggest that a straightforward method to achieve this aim could involve activation of all bonds to SiH_4 with two metal centers to generate $L(H)_2M{=}Si{=}M(H)_2L$ complexes (Figure 1c). The divergent assembly of such platforms ~~should~~ would be well-suited for evaluation of electronic and chemical properties for simple silicides. This report describes the unexpected hydrogen-atom abstraction observed upon reaction of a $Tp"Co^I$ synthon with SiH_4 or $PhSiH_3$ (Tp" = *tris*-3,5-(diisopropylpyrazolyl)borate). Refinement of the ligand design identified a $[PhB(CH_2P^tBu_2)_2(Pz)]^-$ ($[BP_2^{tBu}Pz]$) -ligated cobalt platform for Si—H bond activation and silicide extrusion from SiH_4. Prior work by Thomas and Peters demonstrated that the $[BP_2^{tBu}Pz]$ ligand functions as a stronger donor than related *tris*-phosphine borate ligands $[PhB(CH_2PR_2)_3]^-$, based on cyclic voltametric studies of iron complexes.[22] Thus, the $[BP_2^{tBu}Pz]$ ligand was expected to produce an electron-rich $[BP_2^{tBu}Pz]M$ fragment that more readily activates bonds in silane substrates. Additionally, the diminished steric demand of the $[BP_2^{tBu}Pz]$ ligand relative to $[BP_3^{iPr}]$ was expected to allow ready access to more reactive {MSiM} cores.

RESULTS AND DISCUSSION

Reactions of $(Tp"Co)_2(\mu\text{-}N_2)$ (1) with silanes. Low-valent cobalt complexes supported by a scorpionate ligand were selected for initial evaluation of silicide extrusion from SiH_4. Such ligands have been demonstrated to support closely related 3*d*-metal dinitrogen complexes $(Tp^{R,R'}M)_2(\mu\text{-}N_2)$,[23] which have the possibility to react with SiH_4 to furnish $Tp^{R,R'}(H)_2M{=}Si{=}M(H)_2Tp^{R,R'}$ silicides. The desired starting material $(Tp"Co)_2(\mu\text{-}N_2)$ (**1**) was obtained in good yield (84%) by KC_8 reduction of Tp"CoI.[24]

Surprisingly, treatment of **1** with one equiv of SiH_4 resulted in conversion to two paramagnetic species (Scheme 1a) according to ^{1}H NMR spectroscopic analysis of the reaction mixture, and this observation suggests that the desired silicide $Tp"(H)_2Co{=}Si{=}Co(H)_2Tp"$ was not generated. The major product of the reaction was isolated from cold (–35 °C) ether and identified crystallographically as the mixed-valent Co^I/Co^{II} monohydride $(Tp"Co)_2(\mu\text{-}H)$ (**2**); the hydride ligand was explicitly located in the difference map and refined isotropically in the X-ray solid-state molecular structure. Identification of the second (minor) product $(Tp"Co)_2(\mu\text{-}H)_2$ (**3**) was facilitated by an independent synthesis (*vide infra*). Complex **2** was reliably produced in modest yields by treatment of **1** with one equiv of $PhSiH_3$ (Scheme 1b) in a reaction that generates trace quantities of the dehydrocoupling product $(PhSiH_2)_2$ and small quantities of **3** (11%; see Supporting Information page S3). The outcome of this reaction was unchanged when one equiv of DMAP was added to **1** prior to the addition of $PhSiH_3$, indicating that a prototypical base-stabilized silylene[14,25] of the form $Tp"(H)_2CoSiHPh(DMAP)$ was also not accessible for this system, and that the reaction pathway involves hydrogen atom abstraction.

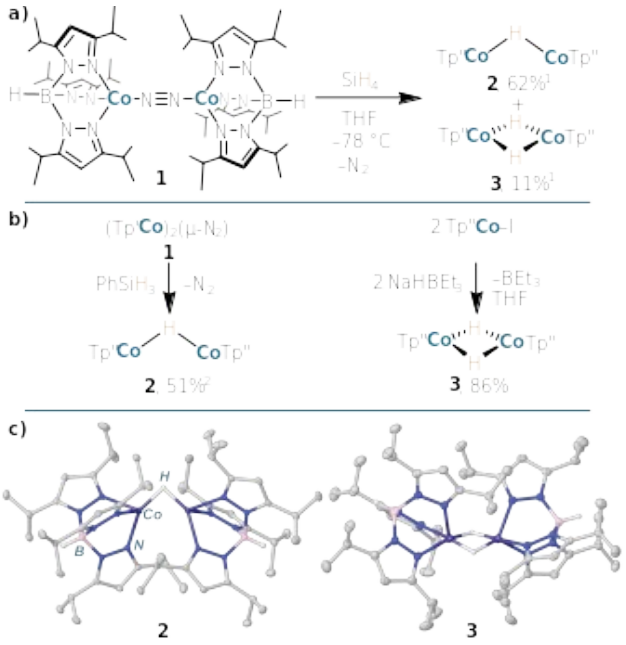

Scheme 1: a) Reaction of **1** with SiH_4, producing a mixture of **2** and **3**. b) Independent syntheses of **2** and **3**. c) Solid-state molecular structures of **2** (left) and **3** (right) with 50% probability thermal ellipsoids drawn. Most hydrogen atoms are omitted for clarity. [1]Yields determined *via* ^{1}H NMR spectroscopy by integration against an internal standard of $(Me_3Si)_2O$. [2]Product mixture contains 11% **3**, *via* ^{1}H NMR spectroscopy by integration against an internal standard of $(Me_3Si)_2O$.

Believing the minor species (**3**) formed upon treatment of **1** with $RSiH_3$ (R = H, Ph) to be the dihydride complex $(Tp"Co)_2(\mu\text{-}H)_2$, an independent synthesis was sought. Treatment of Tp"CoI with $NaHBEt_3$ and subsequent workup afforded plates of the Co^{II}/Co^{II} dimer **3** (Scheme 1b), the identity of which was confirmed by single-crystal X-ray diffraction analysis. The ^{1}H NMR spectroscopic features of **3**

are identical to those of the minor species formed upon reaction of **1** with SiH_4 or $PhSiH_3$. Evans method measurements of the magnetic susceptibility of **3** indicate that it is an $S = 2$ species with $\mu_{eff} = 5.5\ \mu_B$ ($\mu_{S.O.}(4e) = 4.9\ \mu_B$).

As complex **2** is a rare instance of a mixed-valent Co^I/Co^{II} hydride,[26,27] its electronic structure was briefly interrogated. The magnetic susceptibility of **2** ($\mu_{eff} = 6.0\ \mu_B$), measured by the Evans method, suggests an $S = 5/2$ system. However, as samples of **2** are invariably contaminated with small (~10%) quantities of **3**, this value serves only as a rough estimate of the magnetic susceptibility. The perpendicular-mode X-band EPR spectrum (Figure S22) of a frozen 2-methyltetrahydrofuran glass of **2** at 10 K displays a broad axial resonance with $g_{\parallel} = 2.300$, and $g_{\perp} = 2.170$. A large signal at 96 mT supports the assignment of a $S = 5/2$ system, since the effective g value of the signal ($g_{eff} \cong 7$) exceeds possible theoretical effective g values for $S = 3/2$ systems ($g_{max} \cong 6$). It is noted also that a non-Kramers system (*i.e.* a system possessing an integer value of S) such as **3** will not resonate under the conditions of perpendicular-mode EPR, indicating that mixed-valent **2** is responsible for the observed spectrum. In the solid-state, **2** is essentially isostructural to ~~a~~ the closely related $S = 1/2$ Cu^I/Cu^{II} monohydride~~,~~ $(Tp"Cu)_2(\mu\text{-}H)$, reported by Warren *et al*.[28]

A potential explanation for the lack of Co–Si bond formation in **1** is that the comparatively weak ligand-field enforced by the Tp" ligand, relative to $[BP_3^R]$ (R = Ph, ^{i}Pr),[14,29] promotes odd-electron processes (for example, hydrogen atom transfer) as opposed to Si—H oxidative addition, and favors products with high-spin ground states.[23,30] Another factor may be that the Tp" ligand provides insufficient steric protection to support {MSiM} units *in dicobalt systems*. The limited steric demand of the Tp" ligand is manifested in the solid-state molecular structures of **2** (Scheme 1c, left) and **3** (Scheme 1c, right), which display relatively close Co···Co contacts of 2.3771(6) Å and 2.4106(8) Å, respectively. The analogous distance in $[BP_2^{iPr}](PhSiH_2)(H)_2Co{=}Si{=}Co(H)_2[BP_3^{iPr}]$ is 4.1202(5) Å.[14] These observations suggest that the Tp" ligand accommodates much closer packing of metal centers in bimetallic complexes than was observed in $[BP_3^{iPr}]$-based systems.[14]

Phenylsilane activation by $[BP_2^{tBu}Pz]$Co(DMAP). Attention turned to the $[BP_2^{tBu}Pz]$ ligand, as it was expected to provide a stronger ligand field and steric repulsion to enforce a greater metal-metal separation to favor formation of {MSiM} units. Incorporation of the $[BP_2^{tBu}Pz]$ ligand at cobalt was achieved by treatment of $CoCl_2$ with $(Et_2O)Li[BP_2^{tBu}Pz]$ in THF solution. Following workup, $[BP_2^{tBu}Pz]$CoCl (**4**) was isolated as an analytically pure turquoise solid in good (74%) yield. Reduction of **4** with one equiv of KC_8 in THF resulted in a rapid color change to dark brown, and workup produced a dark brown solid identified by X-ray crystallography as the dinitrogen complex $([BP_2^{tBu}Pz]Co)_2(\mu\text{-}N_2)$ (**5**; Scheme 2). Surprisingly, effervescence was observed upon dissolution of **5** in arene solvents or THF. Presumably, this results from the loss of coordinated N_2, as evidenced by changes in the ^{1}H NMR spectra obtained for **5** under ambient conditions, after five freeze-pump-thaw cycles, or under four atm of N_2 (Scheme 2b; see Supporting Information page S5, Figures S33-S40). In contrast, no evidence for related processes was observed for dinitrogen complex **2**.

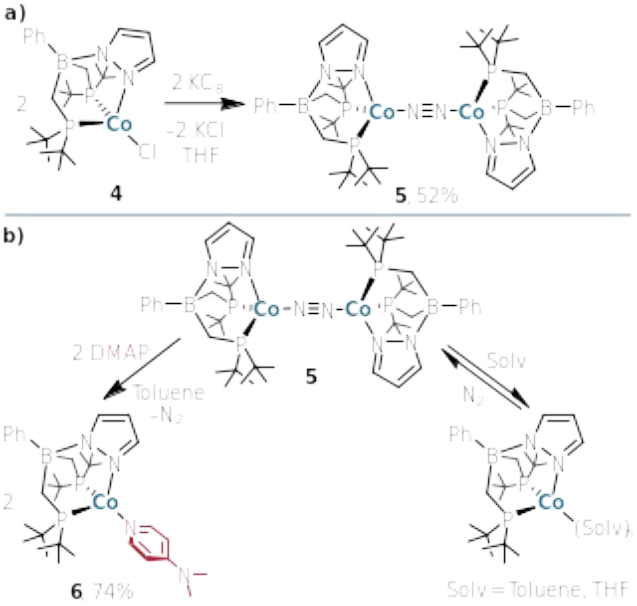

Scheme 2. a) KC_8 reduction of **4** to form **5**. b) Displacement of N_2 from **5** by DMAP and reversible dissociation of N_2 by solvent.

To develop a less labile system, DMAP complex **6** was prepared by treatment of **5** with two equiv of DMAP to give $[BP_2^{tBu}Pz]$Co(DMAP) (**6**; Scheme 2b). This complex was then explored as a synthon or precursor to the 14-electron Co^I fragment $[BP_2^{tBu}Pz]$Co, which was of interest as a potential reaction center for double Si—H bond activations of silanes (*cf.* Figure 1c). The reaction of **6** with $PhSiH_3$ resulted in a rapid color change from dark brown to orange, and ^{1}H and $^{31}P\{^1H\}$ NMR spectra are consistent with the near-quantitative formation of a diamagnetic C_1 symmetrical product, assigned as the base-stabilized silylene complex $[BP_2^{tBu}Pz](H)_2CoSiHPh(DMAP)$ (**7**; **Scheme 3**). Crystals of **7** were obtained by diffusion of $(Me_3Si)_2O$ into a saturated THF solution.

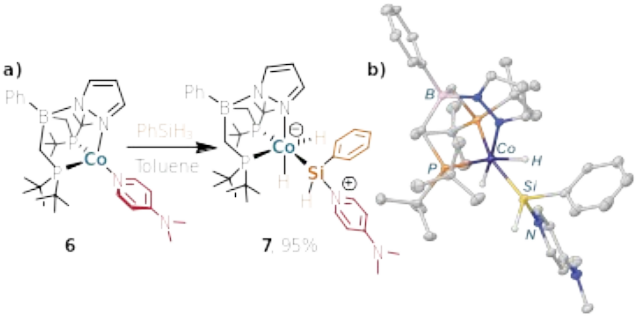

Scheme 3. a) Activation of $PhSiH_3$ by **6** to form base-stabilized silylene **7**. b) Solid-state molecular structure of **7** with 50% probability thermal ellipsoids drawn. Most hydrogen atoms are omitted for clarity.

The solid-state molecular structure of **7**, determined by single-crystal X-ray diffraction, consists of *pseudo*-octahedral complexes of cobalt (Scheme 3b). The hydrogen atoms bonded to cobalt and silicon were located in the difference map and refined isotropically. The silicon atom of the SiHPh(DMAP) ligand lies in the P—Co—P plane, and is associated with a Co—Si bond length of 2.1428(5) Å. This distance is modestly contracted relative to the Co—Si bond

length of 2.1524(8) Å in [BP_3^{iPr}](H)$_2$CoSiHPh(DMAP) (**A**), a closely related analog.[14]

Comparison of the steric maps of the [$BP_2^{tBu}Pz$] and [BP_3^{iPr}] ligands in the analogous complexes **7** and **A**, calculated using SambVca 2.1,[31] shows that the buried volume of [$BP_2^{tBu}Pz$] (%V_{bur} = 75.0)[32] is significantly less than that of [BP_3^{iPr}] (%V_{bur} = 86.8).[33] Thus, the shortened Co—Si bond length of **7** relative to that in **A** may be a manifestation of the diminished steric demand of the ancillary ligand. These features are reflected in the Co—Si Wiberg bond indices (WBIs)[34] for **7** (1.31) and **A** (1.28) based on density functional theory (DFT) calculations at the ωB97X-D3/def2-TZVP//CPCM(benzene) level of theory. The steric demands of both [$BP_2^{tBu}Pz$] and [BP_3^{iPr}] are significantly greater than that of Tp" (%V_{bur} = 59.3).[35]

The multinuclear NMR spectra of **7** and **A** provide further insight into the effect of the ancillary ligands. At 292 K, complex **7** displays resonances consistent with a static C_1 structure, with two distinct 1:1 Co—*H* resonances in the ^{1}H NMR spectrum at δ –28.27 and –11.66 ppm. These resonances correspond to the hydride ligands oriented *trans*- and *cis*- to the N donor atom, respectively, based on multiplet analysis. An analogous trend in δ_H has been observed for the hydride ligands in [(^{i}Pr$_2$PCH$_2$CH$_2$)$_2$NH)]CoH$_3$.[36] Accordingly, the ^{31}P{^{1}H} NMR spectrum of **7** displays two resonances of approximately equal areas (δ 72.0, 81.3 ppm). By comparison, the ^{1}H and ^{31}P{^{1}H} NMR spectra of complex **A** at 292 K are consistent with a *pseudo*-C_3 structure. The ^{29}Si–^{1}H HMBC NMR spectrum of **7** displays a cross-peak at 34 ppm, which correlates to the Si—*H* proton with $^1J_{HSi}$ = 160 Hz. The chemical shift of the ^{29}Si nucleus in **7** is more upfield than that observed for **A** (δ_{Si} = 61 ppm),[14] but remains consistent with a base-stabilized silylene complex.[25,37]

Direct silane activation to form a dicobalt silicide. The synthesis of **7** indicated that the 14-electron [$BP_2^{tBu}Pz$]Co^I fragment might be effective for generation of the silicide [$BP_2^{tBu}Pz$](H)$_2$Co=Si=Co(H)$_2$[$BP_2^{tBu}Pz$] (**8**). Indeed, exposure of a toluene solution of **5** to one equiv of SiH_4 (15% in N_2) resulted in an instantaneous color change from dark red to deep greenish-blue. Following removal of the solvent, crystallization by diffusion of pentane into a saturated THF solution at –35 °C allowed isolation of **8** as an analytically pure crystalline solid in good (84%) yield (eq 1). Notably, this is the first instance of a reaction that produces a symmetrical bimetallic silicide from activation of SiH_4.

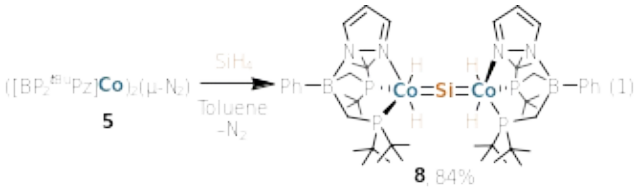

The solid-state molecular structure of **8** (**Figure 2**a) possesses idealized C_2 symmetry; the pyrazole substituents of the two [$BP_2^{tBu}Pz$] ligands are oriented in a staggered *syn* fashion, creating a relatively open pocket that exposes the central silicon atom (Figure 2b).The μ_2-silicon atom displays essentially linear coordination (∠(Co—Si—Co) = 169.07(6)°) and very short Co—Si bond distances (d(Co—Si)$_{ave}$ = 2.058(1) Å). The hydride ligands, located in the Fourier difference map and refined isotropically, are arranged to produce *pseudo*-octahedral coordination about each cobalt center in a manner analogous to that observed for **7**. Notably, the hydride ligands do not form a tetrahedral array about the μ-silicon atom (Figure 2c), indicating minimal "SiH_4" character in the silicide core.[14] The solid-state structure of **8** is superficially similar to that of the previously reported complex [BP_2^{iPr}](PhSiH$_2$)(H)$_2$Co=Si=Co(H)$_2$[BP_3^{iPr}] (**B**), although the latter complex possesses longer central Co—Si bonds (d(Co—Si)$_{ave}$ = 2.074(1) Å).

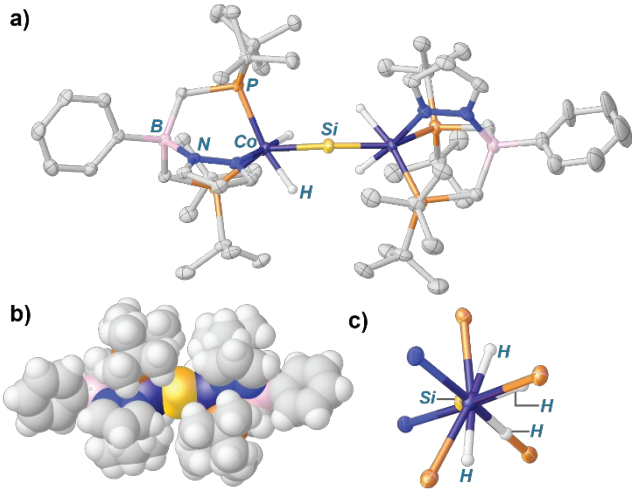

Figure 2. a) Solid-state molecular structure of **8** with 50% probability thermal ellipsoids drawn. Most hydrogen atoms are omitted for clarity. b) Space-filling model of **8**. c) View of **8** along the Co—Co axis, illustrating non-tetrahedral array of hydride ligands about the μ-Si atom.

In the ^{1}H NMR spectrum of **8** at 292 K, the hydride ligand resonances appear as featureless singlets centered at –24.43 and –8.66 ppm. Variable-temperature NMR studies with toluene-d_8 solutions of **8** show that these resonances are readily resolved at sub-ambient temperatures, although fine structure, such as coupling to ^{31}P and ^{29}Si, was not observed due to line-broadening from the nearby quadrupolar ^{59}Co nucleus (I = 7/2).[38] At 203 K, the two Co—*H* resonances give rise to integrations of 2:2 relative to the [$BP_2^{tBu}Pz$] ligand in the ^{1}H NMR spectrum; decoalescence of the phosphorus resonances is also observed, with the ^{31}P{^{1}H} NMR spectrum displaying two broad singlets of approximately equal areas (Figure S52).

The ^{29}Si{^{1}H} NMR spectrum of **8** at 292 K displays a single low-intensity resonance at 274 ppm. This resonance appears at a notably higher field than previously characterized silicides, including **B** (δ = 350 ppm)[14] and Tp*(OC)$_2$Mo≡Si—Mo(CO)$_2$(PMe$_3$)Tp* (δ = 438.9 ppm).[13] The value of J_{HSi} could not be determined from the ^{1}H NMR spectra of **8** at any temperature across the measured range due to broadening of the hydride resonances, while attempts to determine J_{HSi} *via* ^{29}Si—^{1}H HMBC NMR experiments were frustrated by the lack of cross-peaks in the spectrum. Similarly, efforts to record a CP-MAS solid-state ^{29}Si NMR spectrum of **8** were unsuccessful, although this likely arises from the large anisotropy expected for the silicon nucleus,[39–41] as well as the presence of many nearby spin-active (and quadrupolar) nuclei (i.e. ^{1}H, ^{31}P, ^{59}Co).[38]

Computational investigations shed light on the degree of interaction between silicon and the flanking hydride ligands.

The DFT-optimized (non-truncated) geometries of **8** and **B** reproduce the solid-state molecular structures with good accuracy, capturing the Co—Si bond lengths (Δd(Co—Si) < 0.03 Å) and Co—Si—Co angles ($\Delta\angle$(Co—Si—Co) < 3°). The Si···H WBI values for **8** range from 0.42—0.45, while those for **B** range from 0.39—0.42. These values are significantly diminished compared to that of the Si—H bond of the SiHPh(DMAP) substituent in **7** (WBI 0.82) and **A** (WBI 0.82), which serve as useful internal standards for a WBI value associated with a Si—H single bond. This analysis is consistent with minimal Si---H interactions in **8** and **B**; in other words, these silicides are best described as $L(H)_2Co{=}Si{=}Co(H)_2L$ structures, rather than as $LCo(\mu\text{-}SiH_4)CoL$.[42] The Co—Si WBIs for the {CoSiCo} core of **8** (1.47, 1.47) are slightly greater than those of **B** (1.45, 1.44), reflecting the trend established for **7** and **A** of strengthened Co—Si bonding in [$BP_2{}^{t\text{Bu}}$Pz] systems. Also, these bond indices are substantially greater than the Co—Si WBI for the $PhSiH_2$ substituent in **B** (1.07). A scan of the potential energy surface for rotation of the [$BP_2{}^{t\text{Bu}}$Pz]$(H)_2$Co units about the Co—Co axis in **8** was conducted. The energy profile (Figure S13) shows that the molecular geometry found in the solid-state corresponds to the energetic minimum in solution (ΔE_{rot} = 9.0 kcal mol^{-1}) and provides support for the hydride ligand positions determined by crystallography.

Reactions of silicide 8. Complex **8** is a good candidate for investigation of silicide reactivity, given its symmetrical structure and the apparent accessibility of the μ-silicon center. Inspection of the Kohn-Sham orbitals obtained from the DFT-optimized structure of **8** shows that the frontier orbitals (Figure 3) possess significant μ-silicon character. The HOMO of **8** (Figure 3a) is predominantly σ(Co—Si—Co) in character, while the LUMO of **8** (Figure 3b) is dominated by π*(Co—Si—Co) character. The composition of these frontier orbitals indicates that redox and Lewis acid/base transformations are likely to involve the silicide core of **8**.

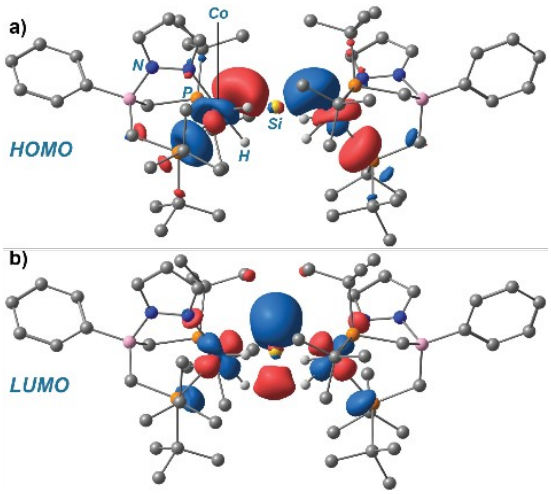

Figure 3. DFT calculated molecular orbitals of **8** rendered at an isovalue of 0.04. Most hydrogen atoms are omitted for clarity. a) HOMO. b) LUMO.

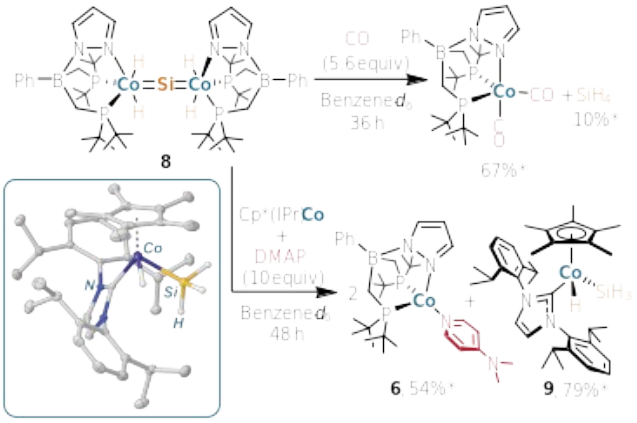

Scheme 4. Displacement of SiH_4 from **8** by excess CO or by treatment with excess DMAP in the presence of Cp*(IPr)Co. *Yields determined *via* ^{1}H NMR spectroscopy by integration against an internal standard of $(Me_3Si)_2O$. *Inset*: Solid-state molecular structure of **9** with 50% probability thermal ellipsoids drawn. Most hydrogen atoms are omitted for clarity.

Treatment of **8** with excess CO resulted in gradual conversion to a new diamagnetic product, identified crystallographically and by independent synthesis as [$BP_2{}^{t\text{Bu}}$Pz]$Co(CO)_2$ (Scheme 4), in 67% yield (based on integration against an internal standard of $(Me_3Si)_2O$). Monitoring the reaction progress by ^{1}H NMR spectroscopy with use of an internal standard indicated that SiH_4 was evolved in low yield (10%). The yield of SiH_4 in this reaction is likely underestimated due to its low solubility in benzene.[43]

The yield of SiH_4 released by treatment of **8** with a Lewis base was more accurately measured by "trapping" SiH_4 using an added complex that activates Si—H bonds. Thus, treatment of **8** with DMAP (10 equiv) in the presence of an unsaturated scavenger complex, Cp*(IPr)Co (Cp* = η^5-C_5Me_5; IPr = 1,3-*bis*-(2,6-diisopropylphenyl)imidazol-2-ylidene),[44] resulted in conversion over 48 h to **6** (54% yield vs. internal standard) and Cp*(IPr)Co(H)(SiH_3) (**9**; 79% yield vs. internal standard; Scheme 4).[45] This reaction is notable in that it demonstrates an unusual SiH_4-transfer between metal centers, despite a lack of "SiH_4 character" in the ground state of the starting silicide.

The silyl hydride complex **9** was prepared independently by treatment of Cp*(IPr)Co in pentane solution with one equiv of SiH_4. The solid-state molecular structure of **9** (Scheme 4, inset) displays a Co—Si bond (d(Co—Si) = 2.2074(7) Å) that is longer than those in **7** and **A**, and does not appear to possess secondary Si—H interactions (d(Si—H) = 2.14(3) Å). The ^{29}Si–^{1}H HMBC NMR spectrum of **9** displays a cross peak with δ_{Si} = –41 ppm and coupling to the silicon bound protons (δ_H = 3.65 ppm, $^1J_{SiH}$ = 162.2 Hz). These structural and spectroscopic features are consistent with the assignment of **9** as a classical silyl hydride complex.

Since silicides are of great significance as catalysts in the Direct Process for the synthesis of Me_2SiCl_2 from methyl chloride, related reactivity for silicide **8** was explored (Scheme 5). Upon introduction of two equivs of MeCl to a benzene-d_6 solution of **8**, no reaction was evident under ambient conditions. However, heating at 60 °C for 24 h resulted in complete consumption of **8** to produce **4** (45% yield vs. internal standard) and trace quantities of $MeSiH_3$ (2%), Me_2SiH_2 (5%), and Me_3SiH (2%; all yields with respect to an

internal standard), according to ^{1}H and ^{29}Si—^{1}H HMBC NMR spectroscopy. Trace amounts of methane and ethane were also evident in the product mixture, consistent with one-electron processes. Following thermolysis, a dark gray powder was deposited in the reaction vessel. An ICP-MS analysis of the solids following aqueous KOH digestion shows the presence of cobalt and silicon, suggesting that the material is a solid-state cobalt silicide. It is unlikely that the material is metallic cobalt, as trace contamination of reactions by solid Co^0 renders solution NMR spectroscopy virtually impossible. Notably, no solids are deposited upon thermolysis of benzene-d_6 solutions containing **8** exclusively.

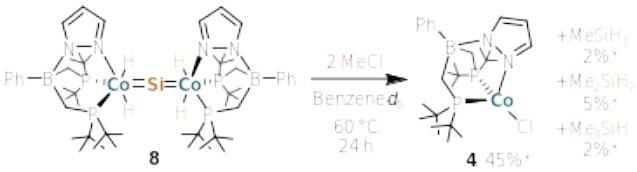

Scheme 5. Reaction of **8** with MeCl, generating **4** and methylhydrosilanes. *Yields determined *via* ^{1}H NMR spectroscopy by integration against an internal standard of $(Me_3Si)_2O$.

Control reactions were conducted to determine the identity of the active species responsible for generating methylhydrosilanes. Heating of a J. Young NMR tube containing SiH_4, MeCl, and benzene-d_6 at 60 °C for 24 h did not result in the formation of any methylsilanes according to the ^{1}H NMR spectrum of the product mixture. Also, complex **4** was treated with MeCl (one equiv) and SiH_4 (0.5 equiv) in benzene-d_6 solution. While no reaction was evident under ambient conditions, heating to 60 °C for 24 h generated traces of $MeSiH_3$ (2% yield vs. internal standard), while most of **4** remained unreacted (39% consumed). Under these conditions, no evolution of methane or ethane was observed by ^{1}H NMR spectroscopy (benzene-d_6). The consumption of **4** under these conditions appears to be related to the deposition of a crystalline blue solid in the reaction vessel, which was identified crystallographically as the zwitterion [κ^2-(P,N)-PhB($CH_2P^tBu_2$)($CH_2P^tBu_2$Me)Pz]$CoCl_2$ (**10**). Complex **10** was independently prepared in good yield (82%) by thermolysis of a toluene solution containing **4** and 1 atm of MeCl (Scheme 6). Notably, addition of 1 atm of MeCl to **8** in benzene-d_6 also led to formation of **10**, albeit in reduced yield (49%; Scheme 6).

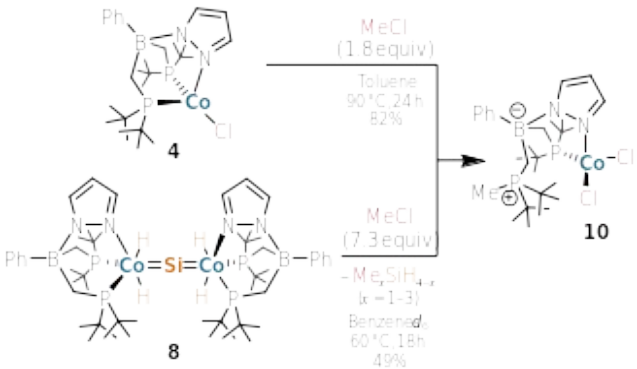

Scheme 6. Reaction of **8** or **4** with excess MeCl, generating **7**.

These experiments point to a complex mechanism involving one-electron redox steps and the presence of at least two active species. However, the cobalt complexes appear to be essential for the formation of functionalized silane products, as thermolysis of a SiH_4/MeCl mixture alone did not result in any conversion of the starting materials (*vide supra*). The selectivity of the reaction between **8** and MeCl for methylhydrosilanes is another unusual feature, as silicide phases typically react with MeCl to produce Me_xSiCl_{4-x} (x = 1–4).[8,7,46] The presence of nearby hydride ligands in **8** likely plays a role in driving the formation of Si—H as opposed to Si—Cl bonds. Additionally, the favorable formation of Co—Cl bonds in complexes **4** and **10** over the course of the reaction may be partly responsible for the observed product distribution.

CONCLUSIONS

A synthon for the 14-electron [BP_2^{tBu}Pz]Co^{I} fragment has allowed observations of double-Si—H bond activations in molecular hydrosilanes. This was shown in the synthesis of base-stabilized silylene complex **7** which introduces two hydride ligands at Co. Most significantly, this fragment provides a rational and direct synthetic route to a bimetallic silicide complex *via* a four-fold Si—H bond activation process. The product of this reaction, silicide complex **8**, possesses close Co—Si contacts and minimal interactions between the μ-silicon center and flanking hydride ligands. Coupled with spectroscopic and computational investigations, these features indicate a distinct lack of "SiH_4 character" in **8**. These investigations indicate that the [BP_2^{tBu}Pz] ligand has a marked influence on the properties of the Co—Si linkages, promoting a greater extent of bonding when compared to related [BP_3^{iPr}] systems; the diminished steric demand of the [BP_2^{tBu}Pz] ligand is likely a critical factor in this regard.

The reaction to produce **8** demonstrates for the first time that SiH_4 can be directly converted to silicide structures without triggering additional rearrangement/decomposition processes in the ancillary ligand. This proof-of-concept reaction opens the door to transformations of SiH_4 to molecular silicides with a broad range of low-valent, unsaturated transition-metal complexes. The subsequent transformations of **8** with small-molecule substrates highlight the non-innocence of the hydride ligands, which readily migrate to form Si—H bonds. This feature, which is not immediately apparent from inspection of the spectroscopic and structural properties of **8**, is potentially exploitable for producing functionalized hydrosilanes. Future efforts are geared toward learning how to control this reactivity for the {CoSiCo} unit.

ASSOCIATED CONTENT

CCDC 2210561—2210572 contain the supplementary crystallographic data for this paper. These data can be obtained free of charge via www.ccdc.cam.ac.uk/data_request/cif, or by emailing data_request@ccdc.cam.ac.uk, or by contacting The Cambridge Crystallographic Data Centre, 12 Union Road, Cambridge CB2 1EZ, UK; fax: +44 1223 336033.

Supporting Information.

Experimental methods, detailed syntheses, details of crystallography, details of calculations, EPR spectroscopy, NMR spectra.

The Supporting Information is available free of charge on the ACS Publications website at DOI: #######.

AUTHOR INFORMATION

Corresponding Author

*tdtilley@berkeley.edu

Notes

The authors declare no competing financial interest.

ACKNOWLEDGMENT

This work was funded by the National Science Foundation under grant no. CHE-1954808 R.C.H. thanks the NSERC of Canada for a PGS-D fellowship. This research used the resources of the Advanced Light Source, which is a DOE Office of Science User Facility under contract no. DE-AC02-05CH11231. Computations were performed using the Tiger cluster at the Molecular Graphics and Computation Facility (MGCF) of the University of California, Berkeley, which is supported by the National Institutes of Health under grant no. NIH S10OD023532, and we thank Dr. Kathleen Durkin and Dr. Dave Small for their advice and expertise on computations. NMR spectra were collected at the College of Chemistry NMR facility, at the University of California, Berkeley which is supported in part by the National Institutes of Health under grant no. S10OD024998; we thank Dr. Hasan Celik and Dr. Alicia Lund for advice and assistance with NMR spectroscopy. Prof. Polly L. Arnold is gratefully acknowledged for use of her X-ray diffractometer.

REFERENCES

(1) Bartschmid, T.; Wendisch, F. J.; Farhadi, A.; Bourret, G. R. Recent Advances in Structuring and Patterning Silicon Nanowire Arrays for Engineering Light Absorption in Three Dimensions. *ACS Appl. Energy Mater.* **2022**, *5*, 5307–5317.

(2) Hasan, M.; Huq, M. F.; Mahmood, Z. H. A Review on Electronic and Optical Properties of Silicon Nanowire and Its Different Growth Techniques. *SpringerPlus* **2013**, *2*, 151–160.

(3) Ramanujam, J.; Shiri, D.; Verma, A. Silicon Nanowire Growth and Properties: A Review. *Mater. Express* **2011**, *1*, 105–126.

(4) Murarka, S. P. Transition Metal Silicides. *Ann Rev Mater Sci* **1983**, *13*, 117–137.

(5) Reader, A. H.; van Ommen, A. H.; Weijs, P. J. W.; Wolters, R. A. M.; Oostra, D. J. Transition Metal Silicides in Silicon Technology. *Rep. Prog. Phys.* **1992**, *56*, 1397–1467.

(6) Johnson, D. C.; Mosby, J. M.; Riha, S. C.; Prieto, A. L. Synthesis of Copper Silicide Nanocrystallites Embedded in Silicon Nanowires for Enhanced Transport Properties. *J. Mater. Chem.* **2010**, *20*, 1993.

(7) Seyferth, D. Dimethyldichlorosilane and the Direct Synthesis of Methylchlorosilanes. The Key to the Silicones Industry. *Organometallics* **2001**, *20*, 4978–4992.

(8) Pachaly, B.; Weis, J. The Direct Process to Methylchlorosilanes: Reflections on Chemistry and Process Technology. In *Organosilicon Chemistry III*; John Wiley & Sons, Ltd, 1997; pp 478–483.

(9) Sysoev, S. E.; Potapenko, D. V.; Ermakov, A. V.; Hinch, B. J.; Strongin, D. R.; Wright, A. P.; Kuivila, C. Chlorosilane Production from Chlorine-Exposed Si(111) 7 × 7 and Cu/Si(111) Surfaces. *J. Phys. Chem. B* **2002**, *106*, 2018–2025.

(10) Roberts, J. M.; Pushkarev, V. V.; Sturm, J. J.; Katsoulis, D. E. Toward a New Direct Process: Synthesis of Methylmethoxysilanes from Dimethyl Carbonate and Pentacopper Silicide. *Ind. Eng. Chem. Res.* **2020**, *59*, 7457–7465.

(11) Schmidt, V.; Wittemann, J. V.; Senz, S.; Gösele, U. Silicon Nanowires: A Review on Aspects of Their Growth and Their Electrical Properties. *Adv Mater* **2009**, *21*, 2681–2702.

(12) Holmes, J. D.; Johnston, K. P.; Doty, C.; Korgel, B. A. Control of Thickness and Orientation of Solution-Grown Silicon Nanowires. *Science* **2000**, *287*, 1471–1473.

(13) Ghana, P.; Arz, M. I.; Chakraborty, U.; Schnakenburg, G.; Filippou, A. C. Linearly Two-Coordinated Silicon: Transition Metal Complexes with the Functional Groups M ≡ Si—M and M=Si=M. *J. Am. Chem. Soc.* **2018**, *140*, 7187–7198.

(14) Handford, R. C.; Smith, P. W.; Tilley, T. D. Activations of All Bonds to Silicon (Si–H, Si–C) in a Silane with Extrusion of [CoSiCo] Silicide Cores. *J. Am. Chem. Soc.* **2019**, *141*, 8769–8772.

(15) Anema, S. G.; Barris, G. C.; Mackay, K. M.; Nicholson, B. K. Improved Syntheses of $M[Fe_2(CO)_8]_2$ (M = Si, Ge or Sn) and the X-Ray Crystal Structure of $Si[Fe_2(CO)_8]_2$. *J. Organomet. Chem.* **1988**, *1988*, 207–215.

(16) Tiel, M. V.; Mackay, K. M.; Nicholson, B. K. Preparation and Structures of Mixed Silicon-Cobalt Carbonyl Clusters with Si-H, Si-O or Si-S Bonds. *J. Organomet. Chem.* **1993**, 79–87.

(17) Ghana, P. *Synthesis, Characterization and Reactivity of Ylidyne and μ-Ylido Complexes Supported by Scorpionato Ligands*; Springer Theses; Springer International Publishing: Cham, 2019.

(18) Thomas, C. M.; Peters, J. C. An η^3-H_2SiR_2 Adduct of $[\{PhB(CH_2PiPr_2)_3\}Fe^{II}H]$. *Angew. Chem. Int. Ed.* **2006**, *45*, 776–780.

(19) Lipke, M. C.; Tilley, T. D. High Electrophilicity at Silicon in η^3-Silane σ-Complexes: Lewis Base Adducts of a Silane Ligand, Featuring Octahedral Silicon and Three Ru–H–Si Interactions. *J. Am. Chem. Soc.* **2011**, *133*, 16374–16377.

(20) Fasulo, M. E.; Lipke, M. C.; Tilley, T. D. Structural and Mechanistic Investigation of a Cationic Hydrogen-Substituted Ruthenium Silylene Catalyst for Alkene Hydrosilation. *Chem. Sci.* **2013**, *4*, 3882–3887.

(21) Lipke, M. C.; Liberman-Martin, A. L.; Tilley, T. D. Electrophilic Activation of Silicon-Hydrogen Bonds in Catalytic Hydrosilations. *Angew. Chem. Int. Ed.* **2017**, *56*, 2260–2294.

(22) Thomas, C. M.; Mankad, N. P.; Peters, J. C. Characterization of the Terminal Iron(IV) Imides $\{[PhBP^{iBu}_2(Pz')]Fe^{IV}{:}NAd\}$. *J Am Chem Soc* **2006**, *128*, 4956–4957.

(23) Cummins, D. C.; Yap, G. P. A.; Theopold, K. H. Scorpionates of the "Tetrahedral Enforcer" Variety as Ancillary Ligands for Dinitrogen Complexes of First Row Transition Metals (Cr-Co): Scorpionates of the "Tetrahedral Enforcer" Variety as Ancillary Ligands for Dinitrogen Complexes of First Row Transition Metals (Cr-Co). *Eur. J. Inorg. Chem.* **2016**, *2016*, 2349–2356.

(24) Han, R.; Looney, A.; McNeill, K.; Parkin, G.; Rheingold, A. L.; Haggerty, B. S. Structural and Spectroscopic Studies on Four-, Five-, and Six-Coordinate Complexes of Zinc, Copper, Nickel, and Cobalt: Structural Models for the Bicarbonate Intermediate of the Carbonic Anhydrase Catalytic Cycle. *J. Inorg. Biochem.* **1993**, *49*, 105–121.

(25) Waterman, R.; Hayes, P. G.; Tilley, T. D. Synthetic Development and Chemical Reactivity of Transition-Metal Silylene Complexes. *Acc. Chem. Res.* **2007**, *40*, 712–719.

(26) Lin, T.-P.; Peters, J. C. Boryl–Metal Bonds Facilitate Cobalt/Nickel-Catalyzed Olefin Hydrogenation. *J. Am. Chem. Soc.* **2014**, *136*, 13672–13683.

(27) Schaefer, B. A.; Margulieux, G. W.; Small, B. L.; Chirik, P. J. Evaluation of Cobalt Complexes Bearing Tridentate Pincer Ligands for Catalytic C–H Borylation. *Organometallics* **2015**, *34*, 1307–1320.

(28) Zhang, S.; Fallah, H.; Gardner, E. J.; Kundu, S.; Bertke, J. A.; Cundari, T. R.; Warren, T. H. A Dinitrogen Dicopper(I) Complex via a Mixed-Valence Dicopper Hydride. *Angew. Chem. Int. Ed.* **2016**, *55*, 9927–9931.

(29) Handford, R. C.; Smith, P. W.; Tilley, T. D. Silylene Complexes of Late 3*d* Transition Metals Supported by *Tris*-Phosphinoborate Ligands. *Organometallics* **2018**, *37*, 4077–4085.

(30) Detrich, J. L.; Reinaud, O. M.; Rheingold, A. L.; Theopold, K. H. Can Spin State Change Slow Organometallic Reactions? *J. Am. Chem. Soc.* **1995**, *117*, 11745–11748.

(31) Falivene, L.; Credendino, R.; Poater, A.; Petta, A.; Serra, L.; Oliva, R.; Scarano, V.; Cavallo, L. SambVca 2. A Web Tool for Analyzing Catalytic Pockets with Topographic Steric Maps. *Organometallics* **2016**, *35*, 2286–2293.

(32) $\%V_{bur}$ was calculated for the [$BP_2^{tBu}Pz$] fragment found in CCDC entry PLACEHOLDER (corresponding to complex **7**) with the following parameters: sphere r = 3.50 Å, H-atoms omitted, scaled bond radii.

(33) $\%V_{bur}$ was calculated for the [BP_3^{iPr}] fragment found in CCDC entry YUPWUE (corresponding to complex **A**) with the following parameters: sphere r = 3.50 Å, H-atoms omitted, scaled bond radii.

(34) Wiberg, K. B. Application of the Pople-Santry-Segal CNDO Method to the Cyclopropylcarbinyl and Cyclobutyl Cation and to Bicyclobutane. *Tetrahedron* **1968**, *24*, 1083–1096.

(35) $\%V_{bur}$ was calculated for the [Tp"] fragment found in **1** with the following parameters: sphere r = 3.50 Å, H-atoms omitted, scaled bond radii.

(36) Rozenel, S. S.; Padilla, R.; Camp, C.; Arnold, J. Unusual Activation of H_2 by Reduced Cobalt Complexes Supported by a PNP Pincer Ligand. *Chem. Commun.* **2014**, *50*, 2612.

(37) Straus, D. A.; Zhang, C.; Quimbita, G. E.; Grumbine, S. D.; Heyn, R. H.; Tilley, T. D.; Rheingold, A. L.; Geib, S. J. Silyl and Diphenylsilylene Derivatives of $(\eta^5\text{-}C_5Me_5)(PMe_3)_2Ru$. Evidence for the Base-Free Silylene Complex $[(\eta^5\text{-}C_5Me_5)(PMe_3)_2Ru{=}SiPh_2]^+$. *J. Am. Chem. Soc.* **1990**, *112*, 2673–2681.

(38) Stone, N. J. Table of Nuclear Magnetic Dipole and Electric Quadrupole Moments. *At. Data Nucl. Data Tables* **2005**, *90*, 75–176.

(39) Kravchenko, V.; Kinjo, R.; Sekiguchi, A.; Ichinohe, M.; West, R.; Balazs, Y. S.; Schmidt, A.; Karni, M.; Apeloig, Y. Solid-State ^{29}Si NMR Study of RSiSiR: A Tool for Analyzing the Nature of the Si–Si Bond. *J. Am. Chem. Soc.* **2006**, *128*, 14472–14473.

(40) Huynh, W.; Conley, M. P. Origin of the ^{29}Si NMR Chemical Shift in R_3Si–X and Relationship to the Formation of Silylium (R_3Si^+) Ions. *Dalton Trans.* **2020**, *49*, 16453–16463.

(41) Gordon, C. P.; Lätsch, L.; Copéret, C. Nuclear Magnetic Resonance: A Spectroscopic Probe to Understand the Electronic Structure and Reactivity of Molecules and Materials. *J. Phys. Chem. Lett.* **2021**, *12*, 2072–2085.

(42) Atheaux, I.; Donnadieu, B.; Rodriguez, V.; Sabo-Etienne, S.; Chaudret, B.; Hussein, K.; Barthelat, J.-C. A Unique Coordination of SiH_4: Isolation, Characterization, and Theoretical Study of $(PR_3)_2H_2Ru(SiH_4)RuH_2(PR_3)_2$. *J. Am. Chem. Soc.* **2000**, *122*, 5664–5665.

(43) O'Neil, M. J. The Merck Index - An Encyclopedia of Chemicals, Drugs, and Biologicals. In *The Merck Index - An Encyclopedia of Chemicals, Drugs, and Biologicals*; Merck and Co., Inc.: Whitehouse Station, NJ, 2001; p 1523.

(44) Andjaba, J. M.; Tye, J. W.; Yu, P.; Pappas, I.; Bradley, C. A. Cp*Co(IPr): Synthesis and Reactivity of an Unsaturated Co(I) Complex. *Chem. Commun.* **2016**, *52*, 2469–2472.

(45) Use of CO gas was avoided in this case due to the documented reactivity of Cp*(IPr)Co with CO to generate Cp*(IPr)Co(CO). See: Andjaba, J.M.; Tye, J.W.; Yu, P.; Pappas, I.; Bradley, C.A. Cp*Co(IPr): synthesis and reactivity of an unsaturated Co(I) complex. *Chem. Commun.* **2016**, *52*, 2469-2472.

(46) Wanandi, P. W.; Glaser, P. B.; Tilley, T. D. Reactivity of an Osmium Silylene Complex toward Chlorocarbons: Promotion of Metal Redox Chemistry by a Silylene Ligand and Relevance to the Mechanism of the Direct Process. *J Am Chem Soc* **2000**, *122*, 972–973.

Insert Table of Contents artwork